

Adapted from Fetter 1988 (Figure 10.20)

Figure 6-3
TCE/PCE Release
Newmark Operable Unit RI/FS Report

LEGEND	
DNAPL	= Dense non-aqueous phase liquid

As depicted in Figure 6-3, NAPLs with densities greater than water such as PCE and TCE can sink through the saturated zone until an impermeable layer, or confining bed, is encountered. The movement of dense NAPLs, or DNAPLs, will follow the slope of the impermeable boundary while a fraction of the DNAPL will go into solution and move in the direction of groundwater flow.

The presence of a DNAPL is generally indicated when the dense organic liquid contaminant concentrations approach 1 percent of the contaminant's solubility limit. However, given the solubilities of PCE (150 to 400 mg/L) and TCE (1,000 and 1,100 mg/L), groundwater concentrations in samples taken from the monitoring wells or municipal wells would have to approach 1,500 $\mu\text{g/L}$ for PCE or 10,000 $\mu\text{g/L}$ for TCE to suggest the presence of a DNAPL layer. The highest concentrations of contaminants were 36 $\mu\text{g/L}$ for PCE and 7 $\mu\text{g/L}$ for TCE (see Table 5-5). In addition, considerable variability in contaminant concentrations would be expected if a DNAPL were present. However, there was little variability in the PCE and TCE concentrations observed in groundwater samples collected from the monitoring wells even though the well screens are all close enough to bedrock to detect any DNAPL pools present at the bottom of the aquifer. Consequently, the presence of DNAPLs, at least in the area of the plume downgradient of the suspected source area monitoring wells, can be reasonably dismissed. Furthermore, it is most likely that PCE and TCE entered the groundwater in an aqueous (i.e., dissolved) phase.

6.3 TRANSPORT MECHANISMS AND PATHWAYS

6.3.1 Transport Mechanisms

The transport or migration of contaminants within the groundwater and into other environmental media (surface water, air, soil, biota), is affected by a number of transport mechanisms and environmental factors. These mechanisms are related to the contaminants' physicochemical properties, including: water solubility, specific gravity, volatility (e.g., vapor pressure), Henry's Law constant and other partition coefficients that define the distribution of chemicals between two phases, and the processes that govern the movement of contaminants in groundwater (advection, dispersion, retardation, transformation). These properties are briefly described below.

Solubility

The solubility of a chemical is defined as the maximum amount of that chemical that will dissolve in pure water at a specified temperature and pH. Solubility is a controlling factor affecting how a contaminant is distributed in surface and groundwater. Highly soluble chemicals tend to remain dissolved in the water column, can be rapidly leached from contaminated soil, and are generally quite mobile in groundwater. Soluble chemicals also tend to be more readily biodegradable than those with low solubility. As shown in Table 6-1, PCE and TCE are slightly to moderately soluble in water and considered moderately mobile.

It should be noted that the solubilities of hydrophobic organics, such as PCE and TCE, increase in the presence of a polar organic solvent, or cosolvent, in the groundwater. This is known as a cosolvent effect. Furthermore, since sorption and solubility tend to be inversely related, any increase in the solubility of the hydrophobic organic would also result in a proportional decrease in sorption.

Solubility can also affect the rate of dissolution of an NAPL layer or pool in an aquifer. As groundwater moves past an NAPL layer or pool (e.g., PCE, TCE), some solvent will dissolve from the surface of the NAPL and diffuse into the groundwater. In time, the groundwater will carry away the solvent. However, in relatively stagnant or low-velocity aquifers, an equilibrium concentration approaching the solvent solubility limit may be established in the groundwater, resulting in very little dissolution of the NAPL layer. The rate of dissolution depends upon a number of factors, including aquifer characteristics (groundwater flow rate, hydraulic gradient, permeability, organic carbon content, fractures, etc.), properties of the solvent (solubility, vapor pressure, sorption potential, etc.), thickness of the NAPL layer, interactions with other contaminants (cosolvent effects, chemical reactions, etc.), and other processes (e.g., biotransformation, contaminant/aquifer interaction).

Specific Gravity

Specific gravity is a unitless value that defines the ratio of the density (e.g., weight per unit volume expressed in g/cm³ or g/ml) of a substance (at a given temperature, commonly 20°C) to the density of water at the temperature of its maximum density (1 g/cm³ at 4°C). Consequently, if the specific gravity

of a substance is less than 1, it will float, and is commonly called a floater; substances having specific gravities greater than 1, such as PCE and TCE, will sink in water and are commonly referred to as sinkers.

Volatility

Volatility, the tendency of a substance to change from the liquid phase to the gaseous phase, is an important parameter to consider when evaluating potential air emissions from a site. Volatilization occurs when molecules of a dissolved or pure substance escape to the ambient air or adjacent gas layer. The relative volatility of a substance is expressed in terms of its vapor pressure. Vapor pressure is the pressure [measured in pounds per square inch (psi) or millimeters (mm) of mercury (Hg)] exerted by a chemical's vapor when in equilibrium with its liquid or solid phase. Vapor pressure is a good indicator of the potential of a chemical to volatilize from land. Chemicals with vapor pressures greater than 10 mm Hg, such as PCE and TCE, are considered highly volatile.

The volatilization rate at the soil/air interface is dependent on the chemical's concentration and physical properties (e.g., solubility, specific gravity, vapor pressure), as well as the properties of the soil (e.g., moisture, temperature, clay and organic content) and adjacent gas layer (e.g., temperature, humidity, wind speed). The rate of volatilization is dependent on the chemical's Henry's Law Constant discussed below, and the chemical concentration and extent of mixing and replenishment in the liquid boundary layer of the liquid/air interface (discussed further below).

Henry's Law Constant

Vapor pressure, solubility, and molecular weight are factors that control volatilization of organic chemicals from water to air. All of these factors are reflected in Henry's Law Constant, H . H is actually a partition coefficient that provides an indication of the tendency of a chemical to partition between the soil gas phase and the soil water in the vadose or saturated zones. Values for H can be

directly measured or calculated from the chemical's water solubility and vapor pressure using the following relationship:

$$H \text{ (atm} \cdot \text{m}^3/\text{mole)} = \text{vapor pressure (atm)} \times \text{MW (g/mole)} / \text{water solubility (g/m}^3\text{)} \quad (6.1)$$

The nondimensional Henry's Law Constant, or H' , is a distribution coefficient that predicts the distribution or ratio at equilibrium of the concentration of a chemical in the gas phase (C_a) to its concentration in the liquid or water phase (C_w) (i.e., $C_a = H' C_w$). Values for H' may be obtained from the literature, experimentally determined, or calculated using the following equation:

$$H' = H \text{ (atm} \cdot \text{m}^3/\text{mole)} / R \text{ (atm} \cdot \text{m}^3/\text{mole} \times ^\circ\text{K)} \times T \text{ (}^\circ\text{K)} \quad (6.2)$$

where: H is the dimensional Henry's Law Constant determined using the relationship described in equation (6.1) above; R is the gas constant ($8.2 \times 10^{-5} \text{ atm} \cdot \text{m}^3/\text{mole} \times ^\circ\text{K}$); and T is the ambient temperature ($^\circ\text{K}$). H' at a standard temperature of 20 to 25°C is equal to $41.7 \times H$.

Chemicals having H values greater than $10^{-3} \text{ atm} \cdot \text{m}^3/\text{mole}$ and vapor pressures greater than 10 mm Hg, such as PCE and TCE, are considered highly volatile chemicals that tend to volatilize fairly rapidly from water.

Partition Coefficients. Partition coefficients describe the distribution of a chemical contaminant between two different media or phases. The coefficients that are particularly important parameters for assessing groundwater transport pathways include the following:

- Octanol/Water Partition Coefficient (K_{ow}). K_{ow} defines the ratio of a chemical's concentration in octanol to that in water. It is representative of a chemical's tendency to partition itself between an organic non-polar phase and an aqueous phase (i.e., its degree of hydrophobicity). K_{ow} is also related to water solubility, soil/sediment adsorption coefficients (see below), and bioconcentration factors for aquatic life. Chemicals with low K_{ow} values (less than 100) are considered relatively hydrophilic and tend to have high water solubilities, small soil/sediment adsorption coefficients, and small bioconcentration

factors for aquatic life. Chemicals with high K_{ow} values (e.g., greater than 10,000) are very hydrophobic and tend to move more readily through biological membranes. PCE ($K_{ow} = 398$) and TCE ($K_{ow} = 195$) fall somewhere in between.

■ Organic Carbon Partition Coefficient (K_{oc}). K_{oc} , a measure of the relative sorption potential of organic chemicals, indicates the tendency of an organic compound to adsorb onto the organic fraction of soils or sediments. K_{oc} is defined as the ratio at equilibrium of the amount of chemical adsorbed per unit weight of organic carbon (μg solute adsorbed/g organic carbon) to the chemical concentration in solution (μg solute/ml solution). The K_{oc} for organic contaminants is essentially independent of site-specific soil properties. Low K_{oc} values indicate greater soil mobility or faster leaching through the soil, high K_{oc} values indicate tight bonding to soils and less mobility. K_{oc} can be determined from the following relationship taken from Hassett et al. (1983):

$$\log K_{oc} (\text{ml/g}) = 0.909 \log K_{ow} + 0.088 \quad (6.3)$$

Values may range from 1 to 10,000,000 ml/g. Based on relatively low K_{oc} values, PCE (283 ml/g) and TCE (148 ml/g) are expected to exhibit low soil adsorption potential and moderate soil mobility.

■ Soil/Water Distribution Coefficient (K_d). K_d is a measure of the tendency of a chemical to partition between water and adjoining soil or sediments. The simplest and most common relationship for expressing adsorption potential is as follows:

$$K_d = C_s/C_w \quad (6.4)$$

where: C_s is the concentration in soil ($\mu\text{g/g}$) and C_w is the concentration in water ($\mu\text{g/ml}$) (Dragun 1988).

If equation (6.4) is normalized on the basis of site-specific soil organic carbon content, much of the variation observed among K_d values over different soils can be eliminated. Normalized, or site-specific, K_d values can be calculated using the following relationship:

$$K_d \text{ (ml/g)} = K_{oc} * f_{oc} \quad (6.5)$$

where: K_{oc} (ml/g) is measured, or estimated using equation (6.3) or other appropriate estimation methods described in Lyman (1990); and f_{oc} is the percent soil organic carbon content (mg organic carbon/mg soil). Since K_d is equal to the product of the chemical's K_{oc} and the fraction of organic carbon in the site's soil, the value of K_d , unlike K_{oc} , may vary considerably in different soils. The f_{oc} for saturated zone soils (50 feet or more below ground surface) in the Newmark study area is estimated to be less than 0.1 percent (Best 1992; Mackay and Vogel 1985; Karickhoff 1981). Using the conservative estimate of 0.1 percent, the K_d values for PCE and TCE for Newmark study area soils are calculated to be 0.283 ml/g and 0.148 ml/g, respectively.

Groundwater Contaminant Migration

The transport of organic contaminants dissolved in groundwater is governed by advection-dispersion processes (e.g., fluid movement, fluid mixing, diffusion), and the geochemical processes that either result in a loss of the contaminant from the plume (transformation or degradation) or delay its movement (retardation and sorption). These processes are briefly discussed below.

Advection, the process of transport resulting from the gross fluid movement of flowing groundwater, is the dominant factor affecting the movement of dissolved contaminants. Groundwater flows from regions of higher water levels to regions where the water level is low, or in the direction of decreasing hydraulic head pressure. The term used to describe the magnitude of this movement is the hydraulic gradient. The velocity of the flow is equal to the product of the hydraulic gradient and the ability of the aquifer medium to transmit water (e.g., ratio of the medium's hydraulic conductivity and porosity). Based on the results of the Newmark Project Flow Model discussed in Section 6.4, the average groundwater velocity in the Newmark contaminant plume study area was calculated to be 358 ft/yr.

1 Dispersion is the processes of molecular diffusion, and mechanical mixing resulting from variations in
2 groundwater velocity (i.e., frictional forces, varying pore sizes, varying path length, velocity gradient
3 variations across the pore space, and the splitting of flow around soil particles), that cause dissolved
4 contaminants to spread as they move with the groundwater. Dispersion and spreading result in
5 contaminant dilution and reduction of contaminant peaks. Consequently, maximum concentrations tend
6 to diminish with increasing distance from the source.

7 Retardation and sorption are the chemical and physical processes that slow or delay the movement of
8 contaminants in groundwater. Some dissolved contaminants may adsorb onto the aquifer material
9 resulting in reduced aqueous phase concentrations, and effectively retarding contaminant movement
10 relative to groundwater flow. For halogenated hydrocarbons such as PCE and TCE, adsorption is
11 affected by the contaminants' hydrophobicity and tendency to adsorb onto organic carbon in the aquifer
12 soils or solids (i.e., soil/water distribution coefficient, or K_d).

13 In a homogeneous aquifer, a linearly retarded contaminant would move at a constant average velocity
14 (V_c) equal to the groundwater's average velocity (V_w) divided by the retardation factor, R_f . R_f is
15 determined by the following relationship:

$$R_f = V_w/V_c = 1 + [(1-n)/n] \rho_s K_d \quad (6.6)$$

17 where: n is the aquifer porosity, assumed to be 30 percent for soils in the Newmark study area
18 (Domenico and Schwartz 1990); ρ_s is the soil particle density, assumed to be 2.65 g/cm³ for soils in
19 the study area (Domenico and Schwartz 1990); and K_d is the adsorption, or distribution coefficient
20 discussed above. The calculated R_f for PCE is 2.75 and 1.91 for TCE. These values are within the
21 expected range of 1 to 10 for most homogenous sand and gravel aquifers that are low in solid organic
22 matter (Mackay et al. 1985), and suggest that the center of mass of the PCE and TCE plume would be
23 expected to move at about 40 to 50 percent of the average velocity of the groundwater.

24 It should be noted that the retardation model defined by equation (6.6) is somewhat simplified. It is

possible that the extent of retardation could vary considerably in space and time due to factors (e.g., contaminant characteristics, presence of other contaminants, aquifer properties etc.) that influence the interaction of a contaminant and the aquifer solids (Mackay et al. 1985).

Biotransformation

Many groundwater contaminants are biologically reactive. Numerous studies have shown that certain aquifers can harbor appreciable populations of metabolically active microorganisms capable of degrading organic contaminants. Depending upon the groundwater or aquifer environment, the biotransformation of contaminants can result in the formation of products that are either less harmful or potentially more toxic and mobile. Potentially, these reactions occur in the aquifer or can be induced in-situ in surface treatment systems supplying required nutrients, substrates, and electron donors/acceptors.

As discussed in Subsection 6.1.2, PCE and TCE can be co-metabolically transformed by methanotrophs, a physiological group of bacteria (e.g., Methylomonas sp., Methylobacter sp., Methylosinus trichosporium, Methylococcus capsulatus) that use (i.e., metabolize) methane as their primary growth substrate, or source of carbon and energy. The reductive transformation under anaerobic conditions favors PCE and the more chlorinated ethylenes, while oxidative transformation under aerobic conditions seems to favor the less chlorinated, short-chained ethylenes.

A number of recent investigations have provided evidence of TCE oxidation by pure cultures of methanotrophs capable of using both methanol and methane as growth substrates. Another study found a bacterial strain capable of degrading TCE that could use either phenol or toluene as a growth substrate, while another strain growing on citrate was reported to degrade PCE as well as TCE (McCarty 1988). Although these studies indicate bacteria other than methanotrophs are capable of co-metabolizing chlorinated alkenes, the methane-oxidizing bacteria are the most common and widely studied of the subsurface bacterial groups.

The primary substrate, methane, is required to supply the major energy requirements for bacterial growth and/or for the activation of enzymes necessary for the biotransformation of the contaminants. Although the transformation of TCE will continue for some time in the absence of methane, it will

1 eventually stop if methane is absent for a prolonged period of time. Methane competitively inhibits the
2 oxidation of TCE since both substrates compete for the same metabolic enzyme, methane
3 monooxygenase (MMO). The proposed transformation mechanism, catalyzed by MMO, is believed to
4 be an epoxidation reaction resulting in the intracellular formation of TCE epoxide which is then extruded
5 from the bacterial cell into the aqueous environment where it undergoes spontaneous abiotic degradation
6 to carbon monoxide, formate, dichloroacetate and glyoxylate (Henry and Grbic-Galic 1991). The
7 relative rate of oxidation appears to increase for compounds containing fewer chlorine atoms per carbon.
8 Highly chlorinated compounds, such as PCE, do not appear to undergo oxidation while less chlorinated
9 compounds such as vinyl chloride are transformed very rapidly. The order of oxidation of a mixture
10 of chlorinated ethylenes, would proceed very rapidly for vinyl chloride; slower for cis-and trans-1,2-
11 dichloroethylene and 1,1-dichloroethylene (DCE); even slower for TCE; and not at all for PCE
12 (McCarty 1988).

13 Transformation under anaerobic conditions, as discussed in Subsection 6.1.2, consists of sequential
14 reductive dehalogenation reactions. The transformation or biodegradation of PCE [PCE to TCE; TCE
15 to the 1,2-DCE isomers (primarily the cis isomer); cis-1,2-DCE to vinyl chloride; and then, perhaps,
16 to ethylene or carbon dioxide] has been demonstrated by several investigators (McCarty 1988). Unlike
17 oxidation, the relative rate of reductive transformation increases for those compounds containing more
18 chlorine atoms per carbon.

19 A multitude of factors affect transformation rates and most are not well understood. The factors include
20 such things as the number and species of microorganisms present, water temperature, pH, interactions
21 between primary and secondary substrates (i.e., methane and PCE and/or TCE), sequential
22 decomposition, sorption, volatilization, microbial toxicity, and transformation reaction stoichiometry
23 (McCarty 1988). In some cases, native microorganisms are incapable of transforming a particular
24 contaminant or need an extended period of acclimation (Mackay et al. 1985). Although it has been
25 fairly well documented that acclimated microorganisms, in numbers necessary to achieve substantial
26 transformation rates, are present in shallow (<18 feet), unconfined aquifers; their presence in deep
27 aquifers has not been fully confirmed.

28 The data generated during this RI fail to provide conclusive evidence that biological transformation may

be occurring and attenuating groundwater concentrations, or otherwise affecting the fate and transport of TCE or PCE in the Newmark groundwater plume. The products of the reductive dehalogenation of PCE (i.e., TCE and cis-1,2-dichloroethylene) were present in some groundwater samples collected from seven monitoring wells (see Table 5-5) and 12 municipal wells (Newmark Wells 1,3, and 4; Electric Drive #2; Parkdale School (W3-2) and (W3-3); Waterman Ave.; 31st St. and Mt. View; 30th St. and Mt. View; Leroy St; 27th St; 17th St), particularly those screened in the deeper anoxic zones. This suggests the likelihood of some subsurface biological transformation. However, the absence of vinyl chloride in all groundwater samples seems to indicate otherwise. The formation of vinyl chloride is expected to accompany the reductive dehalogenation of PCE or TCE. Consequently, some vinyl chloride should have been present at detectable levels in at least some of the groundwater samples. However, this does not preclude the possibility that TCE and vinyl chloride may be undergoing oxidative dehalogenation, with the formation of potential intermediates and end products that are not on the Target Compound List nor included among the analytes of this RI.

6.3.2 Intermedia Transport Pathways

This subsection provides a discussion of the transport of contaminants from the groundwater, or existing contaminant source, to potential points of human or ecological exposure. The potential pathways include volatilization or flux of contaminants from the groundwater to the atmosphere (atmospheric pathway); contaminated water exchange between groundwater and surface water (surface water pathway); and exchange between groundwater and biota (biotic pathway).

Atmospheric Pathway

Based on the results of this focused RI, the transport, or release, of gaseous or airborne particulate contaminants from the vadose and saturated zones underlying the suspected source area is not considered a significant intermedia transport pathway. The analysis of soil cores (see Appendices C and F), collected at different depths during the installation of monitoring wells (MW02 through MW08) in the suspected source area and the results of a soil gas survey conducted in the area of the former disposal trench (see Appendix L) showed no VOCs present in the vadose zone at detectable levels. Consequently,

emissions of contaminated fugitive dusts (i.e., contaminated soil particles) or volatile releases of sorbed contaminants from the unsaturated soils underlying the suspected source area are not considered a potential human or ecological exposure pathway.

Indoor air samples were collected from three suspected source area residences and one control residence. The locations of the four residences are identified in Figure 6-1. A full report describing the sampling protocols and results of the indoor air sampling activities is included as Appendix K. PCE was present in all source area residences at a range of concentrations from 0.56 parts per billion by volume (ppbv) to 0.98 ppbv. TCE was present at two of the source area residences at concentrations of 0.32 ppbv to 0.47 ppbv, but was not detectable above the method detection limit (MDL) of 0.20 ppbv, at the third residence. Both PCE and TCE were detected at concentrations of 0.35 ppbv and 0.25 ppbv, respectively in the indoor air of the control residence located immediately outside the suspected source area. The PCE and TCE concentrations present in the indoor air of these residences were within a range of background levels determined during joint EPA and California Air Resources Board (CARB) surveys (Total Exposure Assessment Methodology or TEAM studies) conducted in the southern California area in 1984 and 1987. The 1987 TEAM study data found 24-hour average PCE concentrations in the indoor air of Los Angeles area residences ranged from 0.21 ppbv to 1.00 ppbv, with a maximum 12-hour concentration of 7.9 ppbv. The 24-hour average TCE concentrations ranged from 0.15 ppbv to 0.82 ppbv, with a maximum 12-hour concentration of 5.23 ppbv.

Surface Water Pathway

The groundwater in the Newmark study area originates from surface water runoff in the San Bernardino Mountains. Surface water flows into the study area across the San Andreas Fault through the outlets of Devil Canyon, Badger Canyon, and Waterman Canyon (Hardt and Hutchinson 1980). Once surface water has passed the base of the San Bernardino Mountains, it flows into percolation basins located downslope of each canyon outlet. Most of the surface water percolates through the alluvial deposits into the groundwater as enhanced groundwater recharge. Data gathered from San Bernardino Valley gaging stations measuring surface-water inflow and outflow support the conclusion that, barring periods of infrequent flooding, most of the surface water entering the valley seeps into the aquifer (Hardt and Hutchinson 1980). Danskin and Freckleton (1989) estimate that 90 percent of the surface water entering

the valley seeps into the groundwater.

The streams and rivers act as natural recharge or discharge points for groundwater and surface water depending on the position of the water table relative to the water level of the streams. Streams filled for short durations during wet winter and spring months percolate downward to the groundwater. During most summer months, the streams are dry and groundwater that flows towards the streams within ten feet of the ground surface is rapidly lost to the atmosphere through evapotranspiration (Hardt and Hutchinson 1980). These study area recharge/discharge points are all located upgradient of the Newmark plume. Consequently, there are no groundwater to surface water discharge points located within the known area of the Newmark plume.

Biotic Pathway

As discussed above, there is no current evidence of PCE or TCE contamination present in surface water, soils, or air capable of supporting biotic populations (e.g., edible crops, livestock, game populations, terrestrial and aquatic animals) that could serve as potential pathways for human or ecological exposure. Therefore, only those biotic populations supported by groundwater pumped from the contaminated Newmark plume would constitute potential pathways for human or ecological exposure.

Based on well pumpage data for the model area obtained from the Western Watermaster (Western Municipal Water District 1986) and the area water agencies (see Subsection 6.4.2), discharge from the groundwater system is limited to municipal wells, private water companies, and mutual water companies that supply domestic drinking water within the model area. These wells constitute the public water system and as such are subject to the requirements of the Safe Drinking Water Act and drinking water MCLs¹, including MCLs for PCE and TCE. These public water system wells currently pumping contaminated groundwater (i.e. Newmark plume groundwater) are treating or otherwise ensuring that

¹ MCLs are the federally-enforceable limits for contaminants in drinking water established under the National Primary Drinking Water Regulations. The MCLs are set by the Office of Drinking Water under the authority of the Safe Drinking Water Act. The State may opt for Primacy Status for drinking water. States which have Primacy Status from EPA must adopt standards which are at least as stringent as federal standards.

the groundwater meets both MCLs and the more stringent state recommended Action Levels. Other than the public water system wells, there are no wells in the model area known to be actively pumping at this time.

Based on the information gathered during this RI, there is no known use of any untreated groundwater from the Newmark plume to support biotic populations. Consequently, biotic populations within the model area are not considered potential human or ecological pathways for exposure to TCE or PCE.

6.4 REVIEW OF PROJECT FLOW MODEL

The primary purpose of the project flow model was to evaluate or screen groundwater extraction and injection alternatives. For the purposes of this Section, the model serves as the basis for estimating contaminant migration. Development of the project flow model consisted of several processes:

- Development of the conceptual model
- Definition of the model area
- Preparation of the input data
- Definition of the grid system
- Calibration of the steady-state and transient-state flow models

The MODFLOW (McDonald and Harbaugh 1988) groundwater flow program was used to simulate the groundwater flow for the Newmark model area. MODFLOW is a groundwater flow program capable only of simulating the advection processes that take place in the groundwater system. Therefore, MODFLOW can only be used to simulate the direction and, to some extent, the rate of transport of dissolved TCE and PCE. PATH3D (Zheng 1991) and SURFER (Golden Software, Inc. 1990) were used as post-processors for the MODFLOW output data. PATH3D, a groundwater path and travel-time program, utilized the input data and unformatted head files of MODFLOW simulations to:

- Create contours of the calculated heads

1 ■ Simulate the pathlines of imaginary particles placed in various areas of the Newmark
2 plume

3 ■ Delineate capture-zones for each extraction scenario

4 SURFER (Golden Software, Inc. 1990) is a graphics program, which utilizes the head contour files
5 created by PATH3D to produce plots displaying the head contours, particle pathlines and locations of
6 the extraction areas.

7 There were two stages in the development and calibration of the project flow model from the
8 MODFLOW program, the steady-state flow model and the transient-state flow model. Transient-state
9 groundwater movement or storage in an aquifer system reflects a change in storage due to the differences
10 in the input and output; in steady-state conditions, however, the change in storage is equal to zero since
11 the input is always equal to the output.

12 The steady-state flow model was simulated and calibrated for the time period between January 1982 to
13 January 1986. The input data and boundary conditions are described in Sections 1.5 and 2.3 of
14 Appendix J. The transient-state flow model was simulated and calibrated for the time period between
15 January 1986 to December 1990. The input data and boundary conditions resulting from the calibration
16 of the steady-state flow model were used as the initial conditions for the transient-state flow model.
17 Some of the input data and boundary conditions (e.g., transmissivities, recharge values) were refined
18 in order to calibrate the transient-state flow model. The calibrated transient-state flow model then
19 became the project flow model which was used for simulation of the extraction scenarios. The measured
20 recharge, streamflow, pumpage, and head values for the January 1986 through December 1990 period
21 were used in the extraction scenario simulations.

6.4.1 Grid System

A grid system with constant grid spacing was constructed for the project flow model, consisting of 3,360 square cells (42 columns and 80 rows). Each cell measures 820.25 feet in both the x- and y-directions. The grid system for the study and model area is displayed in Figure 2 of Appendix J.

6.4.2 Input Data for Project Flow Model

The input data for simulation of the project flow model were arranged into the following seven categories of input files that were read by the project flow model:

- Hydrogeologic layers
- Boundary conditions
- Initial head conditions
- Surface water/groundwater interactions
- Hydraulic conductivity and transmissivity values
- Well pumpage
- Vertical leakance values

Hydrogeologic Layers

The model area consists of igneous and metamorphic basement rock that was downdropped between the San Andreas and San Jacinto Faults. The basin is filled with alluvial deposits which spread around the bedrock hills and reach a thickness of at least 2,100 feet in the southern portion of the model area northeast of the San Jacinto Fault (Hardt and Hutchinson 1980). From here, the basin deposits become progressively thinner towards the northwest and north near the San Bernardino Mountains. [Figure 15 in Appendix J, modified from Hardt and Hutchinson (1980) using additional well information, shows interpreted thickness of the alluvium for the model area; Figure 16 depicts the interpreted surface of the bedrock for the model area.]

1 Several cross-sections were constructed from a detailed analysis of approximately 100 drillers' logs.
2 Interfingering clay lenses that are evident in the individual drillers' logs were grouped together into one
3 middle clay unit that acts as a confining layer for the lower aquifer. Table 1 in Appendix J shows the
4 top and bottom elevations of the middle confining clay unit chosen from each drillers' log. The detailed
5 cross-sections were then compiled into two conceptual cross-sections. In Appendix J, Figure 5 shows
6 the locations of the conceptual cross-sections; Figure 6a represents a north/south cross-section; and
7 Figure 6b represents an east/west cross-section.

8 After further analysis of the cross-sections, the model area was divided into two major aquifers: the area
9 north of Shandin Hills consisting of one unconfined aquifer; and the area just south of Shandin Hills
10 comprised of two aquifers: the upper aquifer, an extension of the unconfined aquifer north of Shandin
11 Hills and the lower aquifer, a separate, confined aquifer. However, for modeling purposes the aquifer
12 north of Shandin Hills was separated into two aquifers by extending the middle confining clay unit
13 through this area at a "zero-foot" thickness and making the lower aquifer approximately 25 feet thick.

14 To further define the aquifer system for model representation, two structure maps were constructed for
15 the middle confining clay unit using the elevations listed in Table 1 of Appendix J. Figure 7 in
16 Appendix J is a structure contour map for the top surface of the middle confining clay unit, and Figure
17 17 is a structure contour map for the bottom surface of the middle confining clay unit. The middle
18 confining clay unit is predominantly clay but includes varying amounts of sand and gravel. The unit
19 is at least 300 feet thick in the central part of the study area near the 7th Street well and thins towards
20 the northern parts of the study area. The top surface of the middle confining clay unit ranges from
21 1,016 feet above sea level at the Darby well just south of the southwest corner of Shandin Hills to
22 approximately 580 feet above sea level in the central part of the model area near Warm Creek.

23 The middle confining clay unit was not modeled as a separate hydrologic layer but rather its thickness
24 was embedded in the vertical leakance values for the overlying unconfined aquifer. The upper model
25 layer (layer 1) is above the middle confining clay unit and the lower model layer (layer 2) is below the
26 middle confining clay unit. The greatest thickness of water-bearing deposits is in layer 2. The bottom
27 elevations for layer 1 correspond to the top elevations of the middle confining clay unit and the top
28 elevations for layer 2 correspond to the bottom elevations of the middle confining clay unit. Since the

designated bottom of layer 1 and top of layer 2 do not coincide in the southern part of the model area, the project flow model recognizes the break between the layers as a middle confining clay unit. The actual thickness of the middle confining clay unit is figured into the vertical leakance values.

Boundary Conditions

The boundary conditions for the model area were defined by the area's geometry, the groundwater/surface water flow conditions, and geologic structures (faults, subsurface groundwater barriers, and impermeable bedrock features). Several boundary condition subroutines that are available in the project flow model were used to represent the actual boundary conditions within the model area. Actual boundary conditions for the model area were represented in the project flow model as no-flow and head-dependent conditions. The boundary conditions are assigned to the individual cells of the model, both for layers 1 and 2.

No-flow conditions were simulated in the model for several impermeable areas that include bedrock hills, mountains, and fault zones. Shandin Hills, Badger Hill, Wiggins Hill, and Perris Hill are bedrock hills that impede groundwater flow within the model area. The San Andreas and San Jacinto Faults were also modeled as no-flow boundaries that border the northeastern and southwestern boundaries of the model area. Figure 18 in Appendix J displays the no-flow cells (impermeable areas). The hydraulic conductivity values for the upper versus lower aquifers are discussed in Section 5.0 of Appendix J.

Head-dependent conditions were simulated using the General-head Boundary package in MODFLOW. Head-dependent conditions were assigned to: eastern and western boundaries of the model area; most upgradient and downgradient positions of the streams, where they enter or leave the model area; and upper aquifer cells, since the streams influence only the upper aquifer. The following are more accurately depicted in Figure 18 of Appendix J:

- The upper cell of Devil Canyon where it intersects the San Andreas Fault
- The upper two cells of Waterman Canyon where it intersects the San Andreas Fault

- 1 ■ The upper eleven cells of Lytle Creek Wash located on the western boundary of the
- 2 model area
- 3 ■ The upper cell of East Twin Creek located on the eastern boundary of the model area
- 4 ■ The upper five cells of the Santa Ana River located on the eastern boundary of the model
- 5 area
- 6 ■ The upper cell of San Timoteo Wash located on the eastern boundary of the model area
- 7 ■ The lower six cells of the Santa Ana River where it crosses the San Jacinto Fault

8 Head-dependent conditions allow for flow to enter or leave a cell i,j,k from an external source. The
9 location of each cell i,j,k is designated by the row (i), column (j), and layer (k). This flow, $Q_{bi,j,k}$, is
10 proportional to the difference between the head in the cell, $h_{i,j,k}$, and the head assigned to the external
11 source, $h_{bi,j,k}$. A linear relationship between flow into the cell and head in the cell is established,

$$12 \quad Q_{bi,j,k} = C_{bi,j,k} (h_{i,j,k} - h_{bi,j,k}) \quad (6.7)$$

13 where: $C_{i,j,k}$ is the conductance between the external source and cell i,j,k (McDonald and Harbaugh,
14 1988). Conductance equals the horizontal hydraulic conductivity times the cross-sectional area of the
15 external source.

16 Several input parameters were needed to simulate the flow across the head-dependent cells:

- 17 ■ Heads for the external source
- 18 ■ Cross-sectional area for the external source
- 19 ■ Horizontal hydraulic conductivity of the external source area

20 Flow values across each head-dependent cell for the upper and lower cells of these streams were
21 calibrated with the 1982 streamflow data for the corresponding gaging station locations. Table 2 in

Appendix J lists the streamflow data that were used in this calibration. Figure 10 in Appendix J illustrates the locations of the gaging stations.

Initial Head Conditions

The project flow model was calibrated for two phases: steady-state and transient-state. Steady-state versus transient-state is described in more detail in Section 2.1 of Appendix J. The steady-state model was calibrated from 1982 to 1986. During this period, the total inflow and outflow of groundwater from the study area did not vary significantly (i.e., groundwater elevations remained fairly consistent) (Hardt and Freckleton 1987; Duell and Schroeder 1989). January 1992 water elevations obtained from Hardt and Freckleton (1987) were used for the initial head conditions. Figures 11 and 12 in Appendix J display the January 1982 initial water elevations for the upper and lower aquifers, respectively.

The transient-state model was calibrated for the period from January 1986 through December 1990. The January 1986 water elevations calibrated for the steady-state model, were used for the initial head conditions of the transient-state model. Figures 19 and 20 in Appendix J display the initial water elevations for the upper and lower aquifers, respectively.

Surface Water/Groundwater Interactions

The General-head Boundary package of the project flow model was used to simulate the groundwater flow into and out of the model area across the upgradient cells of the streams. The River package of the project flow model was used to simulate the effects of flow between the surface-water features and the groundwater system. The package was set up so that surface water recharged the groundwater at all isolated percolation basins and percolation basins connected with the upgradient positions of the streams (Devil Canyon and Waterman Canyon-East Twin Creek). The remainder of the streams were set up as groundwater discharge areas. Figure 18 in Appendix J illustrates the model area portions effected by the streams, percolation basins, and ponds.

Flow between the stream and the groundwater system is characterized by

$$QRIV = CRIV (HRIV - h_{i,j,k}) \quad (6.8)$$

where: QRIV is the flow between the stream and the aquifer, and taken as positive if it is directed into the aquifer; HRIV is the head in the stream; CRIV is the hydraulic conductance of the stream-aquifer interconnection; and $h_{i,j,k}$ is the head at the node in the cell underlying the stream reach. The term for the idealized streambed conductance (CRIV) as it crosses an individual cell is further defined by

$$CRIV = (K L W)/M \quad (6.9)$$

where: L is the length of the stream as it crosses the node; W is the stream width; M is the thickness of the streambed layer; and K is the hydraulic conductivity of the streambed material (McDonald and Harbaugh 1988).

Hydraulic Conductivity Values

Hydraulic conductivity is the quantity of water that will flow through a unit cross-sectional area of a permeable material per unit of time under a unit of hydraulic gradient at a specified temperature. In MODFLOW, hydraulic conductivity values were assigned for both the upper and lower aquifers. Specific-capacity tests performed at municipal wells at the time of installation, were used to quantify the hydraulic conductivity values for the model area. Table 10 in Appendix J lists the hydraulic conductivity values used in the project flow model, and Figure 21 display the calibrated hydraulic conductivity values used in the project flow model for layers 1 and 2.

Faults and impermeable bedrock hills were represented as either no-flow areas or with low hydraulic conductivity values. A hydraulic conductivity of 2.83×10^{-8} ft/day (for upper model layer) and a transmissivity of 2.83×10^{-12} ft²/day (for lower model layer) were used for the San Andreas and San Jacinto Faults and the bedrock hills. The hydraulic conductivity values of the alluvium were used in the areas where streams cross the San Andreas and San Jacinto Faults for the upper modeling layer.

Hydraulic conductivity and transmissivity values of 10.0 ft/day and 400.0 ft²/day, respectively, were used to represent the northwest portion of the Loma Linda Fault and the groundwater barrier that extends south from the Loma Linda Fault (see Figure 21, Appendix J).

Well Pumpage

Well pumpage (ft³/day) was also simulated in the flow model. Most of the discharge from the groundwater system in the model area is from water-supply wells. Well pumpage information for the steady-state model (time period between January 1982 through January 1986) was obtained from the Western Watermaster via Wesley Danskin of the U.S. Geological Survey. Well pumpage information for the transient-state model (time period between January 1986 through December 1990) was obtained from various water agencies:

- City of San Bernardino Water Department
- City of Riverside Public Utilities Department
- West San Bernardino City Water District
- City of Colton Public Works Department
- Meeks & Daley Water Company (now Elsinore Valley Municipal Water Department)
- Riverside Highland Water Company
- East Valley Water District
- City of Rialto Water Division
- Muscoy Mutual Water Company No. 1

The well pumpage data was arranged in average quarterly values for each year. Well pumpage for each municipal well active between January 1986 through December 1990 were used in the calibration of the transient-state model and then used in the predictive simulations for the extracting scenarios. Well pumpage of each municipal well for the last quarter of 1990 (October, November and December) are listed in Table 22 of Appendix J. The location of these wells is shown in Figure 22.

Since the model area is represented by two layers, pumpage for each layer was estimated by well depth,

location, and length of perforations. Pumpage was assigned to the upper model layer for wells perforated only in the upper aquifer. Pumpage for wells perforated only in the lower aquifer was assigned to the lower model layer. Pumpage from wells perforated in both aquifers was prorated, depending on the length of perforations in each aquifer system. The prorated discharge from these wells was allocated to the nearest nodes. As many as seven wells were grouped together to represent the composite pumpage for one model cell.

Vertical Leakance Values

In order to represent the hydrologic connection between the two layers of the model, vertical leakance values were estimated for the middle confining clay unit that separates the upper and lower aquifers in the southern region of the model area. Leakance is the ratio of the vertical hydraulic conductivity of the clay material to the thickness of the middle confining clay unit. In other words, leakance is used to quantify the rate at which water moves vertically through a particular clay unit into the aquifer. Within the model area, some exchange of groundwater between the upper and lower aquifers occurs through the middle confining clay unit.

Initially when leakance values were assigned for the steady-state model, a vertical hydraulic conductivity of 10^{-8} cm/sec (2.83×10^{-5} ft/day) was assumed for the middle confining clay unit (Freeze and Cherry 1979). The thicknesses of the middle confining clay unit ranged from 30 to nearly 300 feet south of Shandin Hills. The resultant leakance values for the middle confining clay unit ranged from 9.43×10^{-7} to 1.00×10^{-7} (ft/day)/ft (see Table 8, Appendix K).

During the calibration of the transient-state model, leakance values for the confining clay unit in the southern region of the study area were increased by factors of 10 to 10^4 . The leakance values for the northern edge of the confining clay unit was increased by approximately a factor of 10^4 ; the leakance values for the middle area of the confining clay unit next to the San Jacinto Fault were reduced by approximately a factor of 10. Figure 12 in Appendix K shows the area of the model area that contains the confining clay unit. Table 11 gives the representative leakance values for selective municipal well areas that were used in the transient-state model, including a leakance value of 0.1 day^{-1} for the northern

region of the model area where no substantial confining clay unit exists. This is shown for areas around the Newmark Wellfield wells, Waterman Avenue well, 30th and Mountain View well, 31st and Mountain View well, and Lynwood well.

6.4.3 Flow Model Results of Existing Conditions

The transient-state flow model, calibrated for the time period from January 1986 through December 1990, was run for a simulated time period of 35 years. This model run enabled the assessment of the influence of existing municipal wells on the Newmark plume, the estimation of the position of the Newmark plume with no remediation enacted and the calculation of groundwater velocities for three areas of the Newmark plume. This predictive run is specifically known as the "no action" scenario (Run 37A0716) discussed in Subsection 13.1.10.

The input data (including the well pumpage) and boundary conditions used in the calibration of the transient-state flow model were applied to Run 37A0716 for the first 5 years of the simulation and repeated in 5-year intervals for 30 additional years.

The existing municipal wells, which were pumping between January 1986 through December 1990, were used through the 35-year simulation. Table 12 in Appendix K gives the locations of the existing municipal wells and their pumping rates for the last quarter of 1990 (October through December) used in the simulation.

PATH3D was used to predict particle pathlines for 3 sets of imaginary particles that totalled 50 imaginary particles. Set 1 contained 6 imaginary particles that were placed upgradient to the Newmark Wellfield wells in a north/south oriented line. Set 2 contained 7 imaginary particles that were placed approximately half-way between the Newmark Wellfield wells and the middle area of the Newmark plume. They were arranged in a north/south oriented line. Set 3 contained 37 imaginary particles that were placed along the outer perimeter of the lower two-thirds of the Newmark plume.

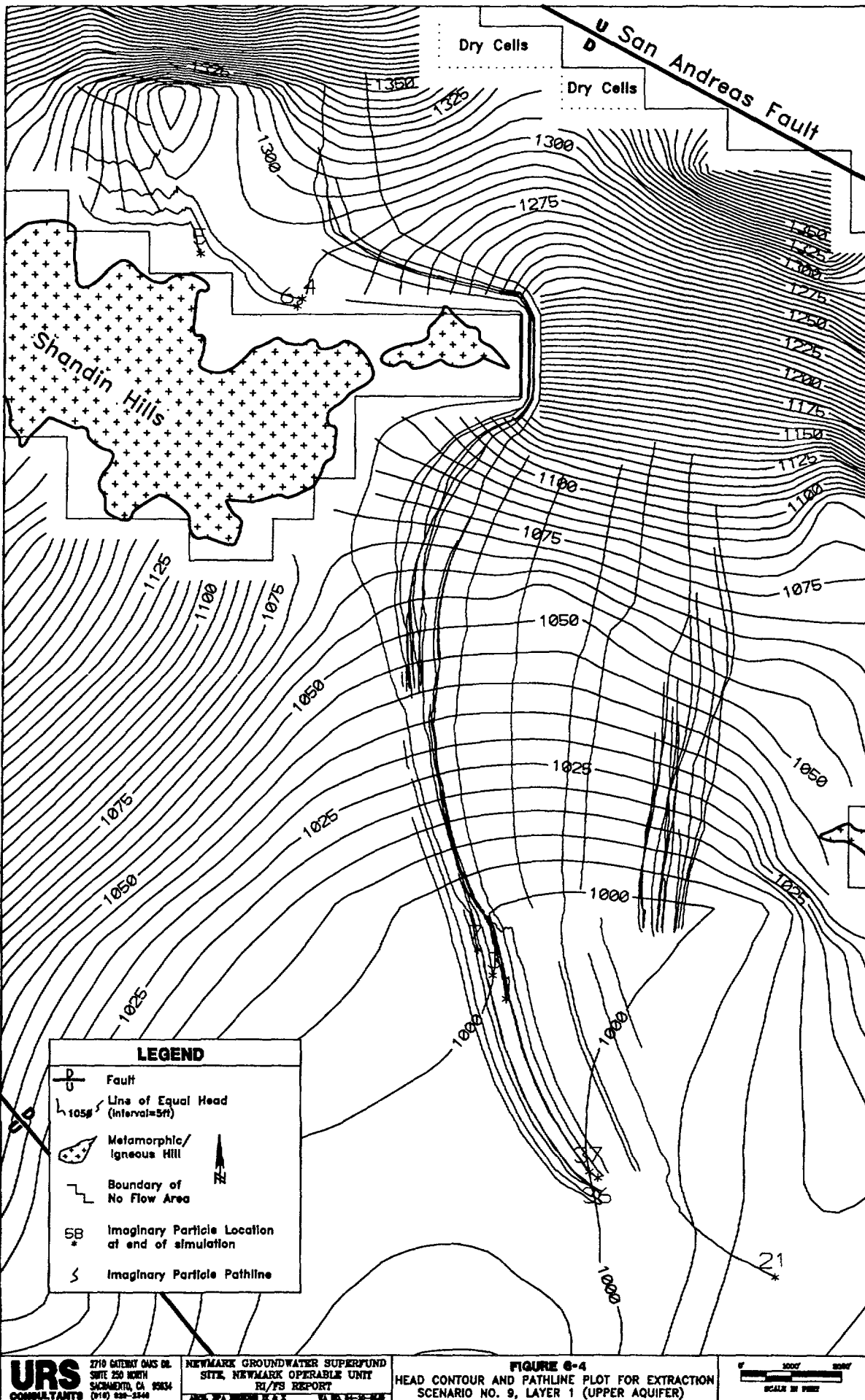
1 SURFER was used to produce plots of the head contours and pathlines created during the application
2 of PATH3D.

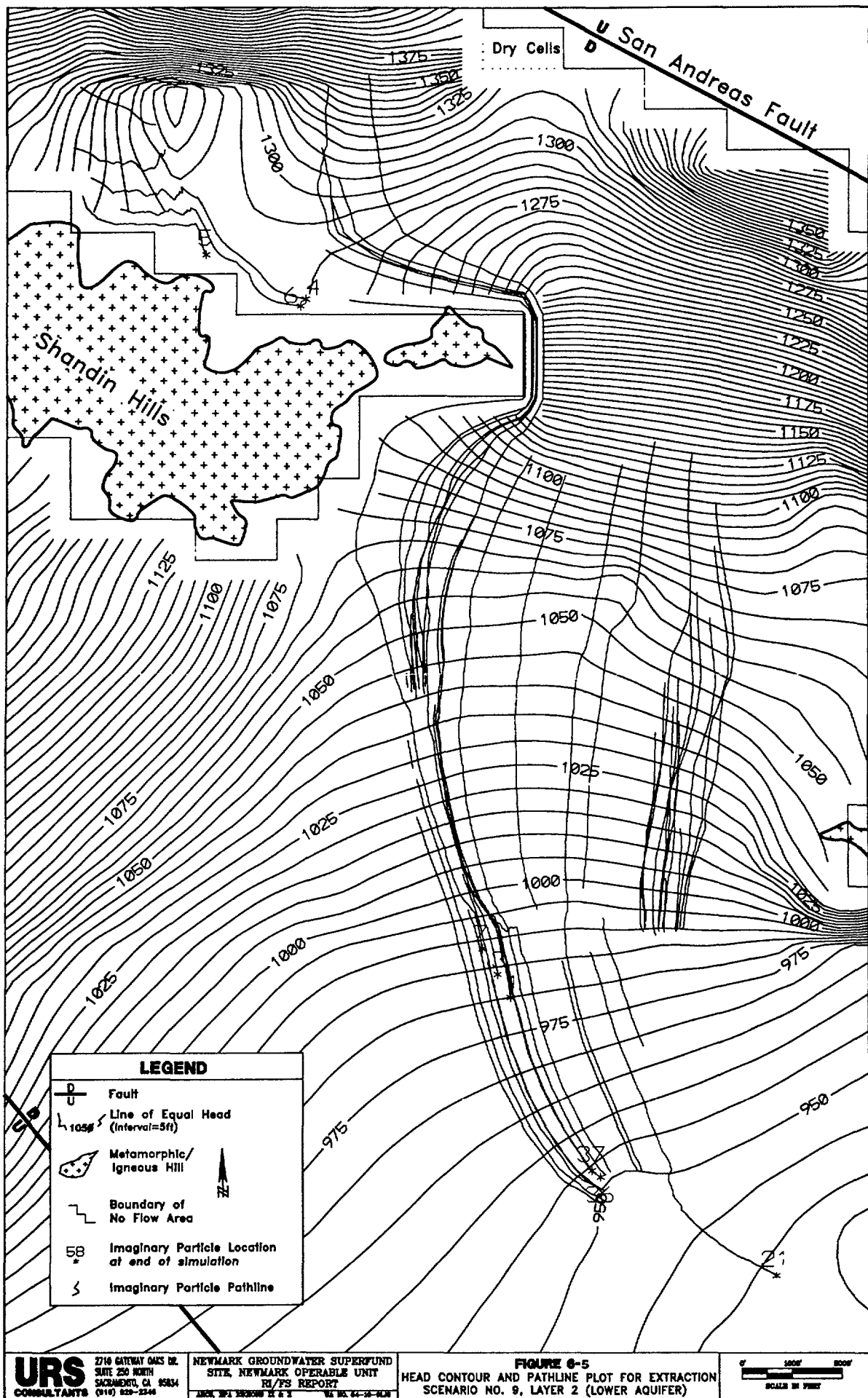
3 Results and Summary

4 The head contour plots for layers 1 and 2 and the PATH3D output file were analyzed. Figures 6-4 and
5 6-5 display the head contour plots for the end of the 35-year simulation for layers 1 and 2, respectively.
6 These figures also display the imaginary particles and their pathlines.

7 The imaginary particles for Set 1 migrated southeast towards a field of several municipal wells. This
8 wellfield is located approximately 2.0 miles southeast of the estimated downgradient edge of the
9 Newmark plume and is in the general area of cells (37,45) and (37,46). The wells in this field are Antil
10 wells no. 2 through 6 (City of San Bernardino), Schueuer (City of Riverside), Garner wells no. 1, 2,
11 4 and 5 (City of Riverside), and East Valley Water District wells no. PL 11A and 12A.

12 Based on the results of the "no action" scenario, the imaginary particles for Set 1 are migrating toward
13 the wellfield described above. However, it is not known at this time if the portion of the Newmark
14 plume represented by the Set 1 imaginary particles would be totally captured by the wellfield. Also, at
15 this time, it is difficult to determine when the Set 1 imaginary particles would reach the downgradient
16 wellfield. Furthermore, since the wellfield described above is located at the eastern edge of the model
17 area, the model area would need to be widened in order to simulate the future movement of the
18 Newmark plume near this wellfield.





URS
CONSULTANTS

2710 GATEWAY OAKS DR.
SUITE 250 NORTH
SACRAMENTO, CA 95834
(916) 820-2240

NEWMARK GROUNDWATER SUPERFUND
SITE, NEWMARK OPERABLE UNIT
RI/FS REPORT
JUNE 2011 VERSION 11.0

FIGURE 6-5
HEAD CONTOUR AND PATHLINE PLOT FOR EXTRACTION
SCENARIO NO. 9, LAYER 2 (LOWER AQUIFER)

0 1000 2000
SCALE IN FEET

At the present time, the Newmark plume is approximately 12,500 feet (2.4 miles) long measured from the northeast edge of Shandin Hills. It is approximately 6000 feet (1.1 miles) wide at its widest point adjacent to the southeast edge of Shandin Hills. Based on the positions of the imaginary particles and assuming no retardation of the contaminant velocities, the extent of the Newmark plume will be approximately 20,000 feet (3.8 miles) long from the northeast edge of Shandin Hills after 35 years of migration. It will be approximately 6500 feet (1.2 miles) wide at its widest point adjacent to the southeast edge of Shandin Hills. Therefore, according to the results of the project flow model as shown in Figures 6-4 and 6-5, the Newmark plume will migrate approximately 7500 feet (1.4 miles) downgradient and widen approximately 500 feet (0.09 mile) in 35 years.

The following four groups of existing water-supply wells within the Newmark plume captured imaginary particles during the simulation and, therefore, may have an influence on the plume.

- 1) The North E St. and 27th St. wells captured particles on the westside of the plume (southeast edge of Shandin Hills).
- 2) The 23rd St. well also captured particles on the westside of the plume.
- 3) The 16th and 17th St. wells captured particles in the center approximately 2000 feet north of the extraction wells located at the downgradient edge of the plume.
- 4) The Gilbert St. well captured particles located in the southeast portion of the plume.

The North E Street, 27th Street and 23rd Street wells contained very small amounts of contamination during the latest sampling. The 16th and 17th Street wells had slightly higher concentrations of contaminants. The Gilbert Street well has had no detectable contamination to date.

1 Based on the present configuration of the model and pumping values from 1987-1991 data, the most
2 conservative model projections estimate that the Newmark plume edge will reach the Gilbert Street well
3 area circa 1995. If remained unchecked, the plume is predicted to reach the Seventh Street well in
4 approximately 15 years and the Antil pumping facility in approximately 24 years. Figure 6-6 depicts
5 particle flow-paths and head contours in the plume's lower two-thirds area. The model indicates that
6 the plume as a whole is generally moving towards the Antil facility and will continue to migrate and
7 affect the facility once it has arrived.

8 Groundwater velocities were calculated for three areas of the Newmark plume: the Newmark Wellfield
9 well area, the middle area, and the lower two-thirds area. The groundwater velocities were represented
10 by the velocities of the imaginary particles that were placed in the three areas of the Newmark plume.
11 The velocity of an imaginary particle equals the travel-distance divided by the travel-time. Imaginary
12 particles that were not affected by the boundary conditions of the project flow model and plotting
13 limitations of SURFER and PATH3D were used to calculate average groundwater velocities for the three
14 areas of the Newmark plume. Table 6-2 presents the average groundwater velocities calculated for the
15 three areas.

16 The estimated average groundwater velocity for the Newmark plume area is a simple arithmetic average.
17 The groundwater velocities for the three areas were weighted evenly in the calculation for the following
18 reasons:

- 19 ■ The project flow model is simply a computer model and, therefore, groundwater
20 velocities provided by the project flow model are estimates or averages;
- 21 ■ It is not known how the groundwater velocities estimated for the three areas of the
22 Newmark plume compare with actual field conditions since they have not been measured.
23 Therefore, the calculated velocities could not be verified but represent the best possible
24 estimates until actual measurements are conducted; and

